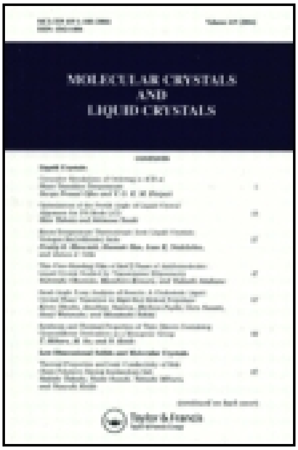

Molecular Crystals and Liquid Crystals Science and Technology. Section A. Molecular Crystals and Liquid Crystals
Publication details, including instructions for authors and subscription information:
http://www.tandfonline.com/loi/gmcl19

Optical Second-Harmonic Generation at Selective Reflection Band of The SmC* Phase

I. Drevenšek Olenik [a b] & M. Čopič [a b]
[a] Department of Physics, University of Ljubljana, Jadranska 19, Ljubljana, Slovenia
[b] J. Stefan Institute, Jamova 39, Ljubljana, Slovenia

Version of record first published: 24 Sep 2006

Mol. Cryst. Liq. Cryst., Vol. 320, pp. 265–275
Reprints available directly from the publisher
Photocopying permitted by license only

Optical Second-Harmonic Generation at Selective Reflection Band of the SmC* Phase

I. DREVENŠEK OLENIK and M. ČOPIČ
Department of Physics, University of Ljubljana, Jadranska 19, Ljubljana, Slovenia
J. Stefan Institute, Jamova 39, Ljubljana, Slovenia

The process of optical second harmonic generation (SHG) in a slab of the helically modulated SmC* material is analysed for a case when the SHG frequency is in the vicinity or inside the region of the selective reflection band. The analysis bases on the numerical solutions of the nonlinear wave equation. Various possible phase matched combinations of the optical eigen-modes are discussed and the dependence of the SHG intensity on the optical frequency and sample thickness is given.

Keywords: optical second harmonic generation, ferroelectric liquid crystals

INTRODUCTION

During the last decade several techniques have been developed to construct various periodic dielectric structures on the scale of optical wavelengths[1]. These media, known as photonic band materials, exhibit optical properties very similar to the properties of electrons in periodic lattices[2]. Their optical dispersion spectrum exhibits a characteristic band structure with "forbidden" gaps which are polarization dependent. As a boundary between the neighboring layers in periodic dielectric structures is usually very sharp, several reciprocal lattice vectors have to be taken into account when solving the Maxwell equations in such structures. This requires quite complex computational procedures even in a case of linear optical phenomena. Consequently the nonlinear optical processes, like optical second-harmonic generation (SHG), are analyzed mostly only qualitatively with assuming several approximations[3].

Chiral liquid crystalline phases, on the contrary, represent an example of inherent periodic dielectric structures with a smooth continuous modulation of the optical properties. The set of their reciprocal lattice vectors is small and for propagation along the axis of the helical modulation the optical eigenmodes can be described with a relatively simple analytic expression[4,5]. This allows that also the nonlinear optical processes can be readily treated in more exact manner.

Recently we have developed a procedure to calculate the exact optical second harmonic field generated in a slab of the helically modulated SmC* material. The plane optical waves are supposed to propagate along the direction of the helical axis and power depletion of the fundamental waves is neglected. The procedure, similar to the Berreman 4x4 formalism, is described elsewhere[6]. In this paper we present and discuss the results of this procedure for a specific case when the second harmonic frequency is in the vicinity of the selective reflection band. This case is very interesting as, accordingly to the previous approximate calculations[7-11], some additional enhancement of the SHG process can appear when the SHG frequency is near the reflection band edge. It also corresponds to the experimental situation of Kajikawa et al. and Furukawa at al. who have recently measured the SHG signal from the helical SmC* samples and observed some effects analogous to the effects in distributed feedback laser systems[12,13].

THEORY

The optical properties of the chiral SmC* structure are described by the local C_2 symmetry of the mesophase. In compliance with this symmetry the optical dielectric tensor ε has 3 different principal values and the tensor of the second-order nonlinear optical susceptibility $\chi^{(2)}$ has 4 independent non-zero components (assuming Kleinman's symmetry). The direction of the 2-fold axis, which is parallel to the smectic layers, is helically modulated when one moves from one smectic layer to another. The periodicity of this modulation is of order of magnitude of optical wavelengths. For optical beams propagating along the helical axis ($\bar{e}_z$ axis) the transverse electric field of the eigen-modes is analogous to the optical eigen-modes of the cholesteric phase[4,5,14]. These are the Bloch-wave like fields

$$\vec{E}_k^{tr} = E_{k,+}\vec{e}_+ + E_{k,-}\vec{e}_- = \left(\frac{-f_k e^{i(k+q_o)z}}{\sqrt{1+|f_k|^2}}\right)\left(-\frac{\bar{e}_x+i\bar{e}_y}{\sqrt{2}}\right)+\left(\frac{e^{i(k-q_o)z}}{\sqrt{1+|f_k|^2}}\right)\left(\frac{\bar{e}_x-i\bar{e}_y}{\sqrt{2}}\right) \quad (1)$$

where $\bar{e}_\pm = \mp(\bar{e}_x \pm i\bar{e}_y)/\sqrt{2}$ denote the unit vectors of the circular base. The dispersion relation $k(\omega)$ and the polarization factor f_k of these fields are given by

$$k = \pm\left((k_o^2\bar{\varepsilon}+q_o{}^2)\pm\sqrt{4k_o^2\bar{\varepsilon}q_o{}^2+\alpha^2k_o^4}\right)^{1/2}, \quad (2)$$

and

$$f_k = \frac{(k-q_o)^2-k_o^2\bar{\varepsilon}}{\alpha k_o^2} = \frac{\alpha k_o^2}{(k+q_o)^2-k_o^2\bar{\varepsilon}} \quad (3)$$

The introduced parameters k_o, q_o, $\bar{\varepsilon}$ and α are

$$k_o = \frac{\omega}{c}\ ,\ q_o = \frac{2\pi}{p}\ ,\ \bar{\varepsilon} = \frac{1}{2}\left(\varepsilon_{11}+\varepsilon_{22}+\frac{(\varepsilon_{33}-\varepsilon_{11})\varepsilon_{11}\sin^2\theta}{\varepsilon_{11}\sin^2\theta+\varepsilon_{33}\cos^2\theta}\right),\ \alpha = \bar{\varepsilon}-\varepsilon_{22}, \quad (4)$$

where ω is the frequency of optical field, c is the speed of light in vacuum, p is the helical pitch, θ is the molecular tilt angle and ε_{ii} are the principal values of the optical dielectric tensor ε.

Two of the four eigen-modes as given by Eq. (1) correspond to optical beams which propagate in the direction of the $\bar{e}_z$ axis and the other two to the equivalent beams that propagate in the direction of the -$\bar{e}_z$ axis. In the dispersion spectrum shown in Fig.1 the corresponding branches are labeled as branches 1, 2 and 3, 4 respectively. The main characteristic of the dispersion spectrum $k(\omega)$ is the "forbidden" gap inside which two eigen-values of k, as found from Eq. (2), become imaginary. In the region of this gap the circularly polarized optical waves which match with the handedness of the SmC* helix can not propagate, but experience Bragg reflection from the structure. The gap, known also as the selective reflection band, extends in the frequency interval from $(1-(\alpha/2\bar{\varepsilon}))\omega_B$ to $(1+(\alpha/2\bar{\varepsilon}))\omega_B$, where $\omega_B = q_o c/\sqrt{\bar{\varepsilon}}$ is the Bragg frequency.

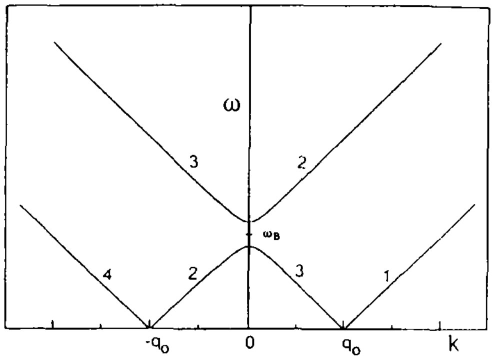

FIGURE 1 The dispersion relation for optical eigen-waves propagating along the helical axis in a SmC* liquid crystal.

Consider a homeotropically aligned slab of the SmC* material immersed in an isotropic surrounding medium. The plane monocromatic optical waves $\vec{E}_l = \vec{E}_{l0}e^{ik_0z-i\omega t}$ and $\vec{E}_r = \vec{E}_{r0}e^{-ik_0z+i\omega t}$ enter the slab from the left (forward) and from the right (backward) side in the normal direction, that is along the axis of the helical modulation. These ingoing fundamental waves are partially reflected and partially transmitted through the slab. The generation of the second harmonic optical field within the slab is described by the non-linear wave equation

$$\nabla\times\nabla\times\vec{E}(z,2\omega) - \left(\frac{2\omega}{c}\right)^2 \varepsilon\, \vec{E}(z,2\omega) = \left(\frac{2\omega}{c}\right)^2 \chi^{(2)}:\vec{E}(z,\omega)\vec{E}(\vec{r},\omega), \quad (5)$$

where $\vec{E}(z,\omega)$ and $\vec{E}(z,2\omega)$ denote the internal optical fields. Relation between them and the external fields is given by the boundary conditions which require that the transverse field components and their spatial derivatives are continuous across the surfaces of the slab, that is at the planes $z=0$ and $z=L$, where L is the thickness of the slab.

Eq. (5), together with the above mentioned boundary conditions for the fundamental and the second harmonic fields in general results in a system of 16 non-linear differential equations. Recently we have developed a (numerical) procedure to calculate the exact solutions of this system in the non-depletion limit, that is neglecting the power depletion of the fundamental beams. The procedure gives the amplitude and the polarization of the outgoing second harmonic waves $\vec{G}_l = \vec{G}_{l0}e^{-2ik_0z+2i\omega t}$ and $\vec{G}_r = \vec{G}_{r0}e^{2ik_0z-2i\omega t}$ for arbitrary incident fields $\vec{E}_l$, $\vec{E}_r$ and presumed material parameters. The results given in this paper were obtained with the material parameters: $\theta = 0.5$, $\varepsilon_{11}(\omega) = 2.28$, $\varepsilon_{22}(\omega) = 2.281$, $\varepsilon_{33}(\omega) = 2.86$ and $\varepsilon_{11}(2\omega) = 2.30$, $\varepsilon_{22}(2\omega) = 2.301$, $\varepsilon_{33}(2\omega) = 2.88$, while all the non-zero components of the $\chi^{(2)}$ have been taken to be 1. The thickness of the slab L was measured in the units of the helical pitch p. For these reasons the given values for the SHG intensity are only comparative.

RESULTS

We started the examination of the problem with the most usual situation when the linearly polarized fundamental wave enters the SmC* slab from one side only, that is the case $\vec{E}_{l0} = \vec{e}_x$, $\vec{E}_{r0} = 0$. Fig. 2 shows the frequency dependence of the intensity $I_{2\omega}$ of the transmitted $(\vec{G}_r)$ and reflected $(\vec{G}_l)$ second harmonic waves. The grey shadowed band in the figure denotes the interval of the fundamental frequencies ω at which the corresponding SHG frequencies 2ω fall into the region of the "forbidden" gap. The thickness of the sample is $L = 100/q_o$. The SHG intensity significantly increases when 2ω is in the vicinity of the gap. The width of the peak, with the maximum located within the gap, is relatively large and extends far out of the gap region. Very similar SHG intensities appear in the reflected as well as in the transmitted direction.

The generated second harmonic radiation results from non-linear interaction of various pairs of the excited fundamental eigen-modes $\vec{E}_k^{tr}(z,\omega)$. Fig. 3 shows to which amount different pairs (combinations) of the fundamental eigen-modes contribute to the total transmitted SHG intensity.

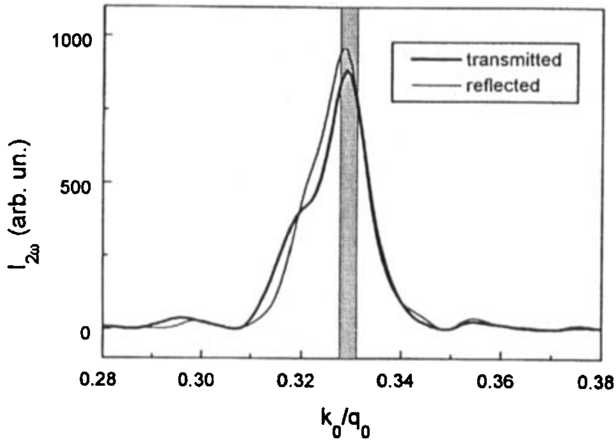

FIGURE 2 The dependence of transmitted and reflected SHG intensity on the frequency of the fundamental beam.

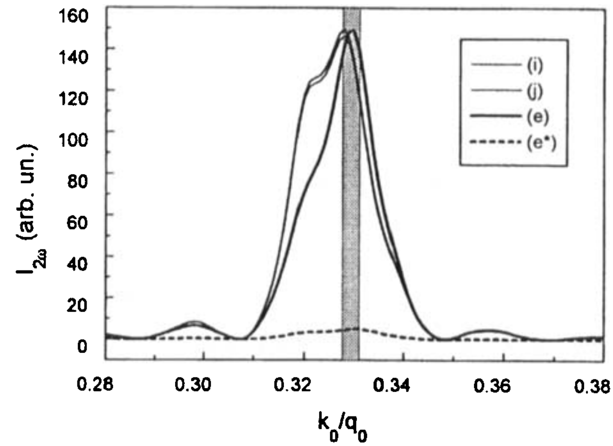

FIGURE 3 The contributions from various eigen-mode combinations to the transmitted SHG intensity.

It is apparent that the important contributions arise only from these combinations that can be phase matched in the frequency region near the band gap. The phase matching of the second harmonic and fundamental optical eigen-modes in the helical SmC* structure is realized when the mismatch of the corresponding Bloch wave vectors Δk is zero, that is when

$$\Delta k = (k_i(2\omega) - k_j(\omega) - k_l(\omega)) = 0, \tag{6}$$

where k_i, k_j, k_l denote any of the four eigen-values as given by eq. (2) and accordingly presented in the Fig. 1 [6,9,10]. For the SHG frequency in the region $2\omega \approx \omega_B$ there are three combinations that can satisfy Eq. (6). These are the combinations

$$\begin{aligned} &k_1(2\omega) = (k_1(\omega) + k_3(\omega)) \approx 2q_o && \text{(e)},\\ &k_2(2\omega) = (k_2(\omega) + k_3(\omega)) = 0 && \text{(i)},\\ &k_2(2\omega) = (k_1(\omega) + k_4(\omega)) = 0 && \text{(j)}, \end{aligned} \tag{7}$$

which are labelled as combinations (e), (i) and (j) respectively. The labelling is set accordingly with our previous work related to the problem of the phase matching of the optical SHG in the SmC* phase in general[6]. The combinations (i) and (j) could in principle be realized when the SHG frequency 2ω coincides with the lower or the upper edge of the "forbidden" gap. But it can be shown that due to the symmetry of the $\chi^{(2)}$ only the SHG eigen-field corresponding to one of the gap edges can be generated[10]. For the SmC* materials with the positive dielectric anisotropy (as assumed in our numerical procedure) the SHG field coincides with the lower band edge. Looking at Fig. 3 one can notice that for the slab of the thickness $Lq_o = 100$ all the three combinatioηs (e), (i) and (j) contribute to the total transmitted SHG intensity quite the same amount. Also the widths of the corresponding peaks are very similar. The contribution from the combination (e*), which is an inverse of the combination (e) with the branches 2 and 4 of the dispersion spectrum and can not be phase matched for the forward propagating SHG beam, is given as a dashed line denoting the background from other combinations.

The realization of the SHG combinations (e), (i) and (j) requires the fundamental optical waves propagating in the forward as well as in the backward direction. Supposing that in the experiment the fundamental optical beam enters the slab from one side only, the needed backward propagating fundamental beam is generated by reflection on the back surface of the slab. For that reason the power transformation to the outgoing SHG beam is quite low. If instead the counter propagating fundamental beams are used the total

SHG power is increased for about a factor of 50 with respect to the case described by the Fig. 2.

The second problem that has been examined was a dependence of the SHG signal on the thickness of the slab L. This analysis was focused on the behaviour of the eigen-wave combinations (e) and (i). The combination (e) represents the non-linear interaction process where the resulting SHG field of the frequency $2\omega \approx \omega_B$ corresponding to the branch 1 on the dispersion spectrum of the Fig. 1 is generated. As this branch does not exhibits any anomaly in the region of the "forbidden" gap a usual dependence $I_{2\omega} \propto L^2$ for the phase matched SHG process is expected. The combination (i) on the contrary represents the process where the SHG field corresponding to the gap exhibiting branch 2 is formed and therefore some anomalies are expected. Fig. 4 shows the frequency dependence of the SHG intensity corresponding to the combinations (e) and (i) for three different sample thicknesses. The peak related to the combination (e) indeed increases proportionally to the L^2, while the peak corresponding to the combination (i) grows much faster. Accordingly it is becoming also more and more narrow with respect to the peak from the combination (e). The position of the peak from the combination (e) practically does not change with the sample thickness while the position of the peak from the combination (i) is moving toward the band edge, that is toward the phase matching point. The peak related to the combination (i) therefore appears at $\Delta k \neq 0$.

The dependence of the enhancement ratio, that is the ratio of the maximum possible $I_{2\omega}$ values related to the eigen-wave combinations (i) and (e), on the sample thickness L is shown in Fig. 5. For $Lq_o >> 100$ the enhancement on average increases with the sample thickness approximately as L^2. This means that the overall SHG signal corresponding to the combination (i) increases as $I_{2\omega}(i) \propto L^4$, in agreement with the previous predictions achieved by the analytical analysis of this problem[9-11]. But as the intense peak related to the combination (i) is very narrow, several mutual interference effects between the fundamental and the SHG eigen-waves within the slab significantly vary

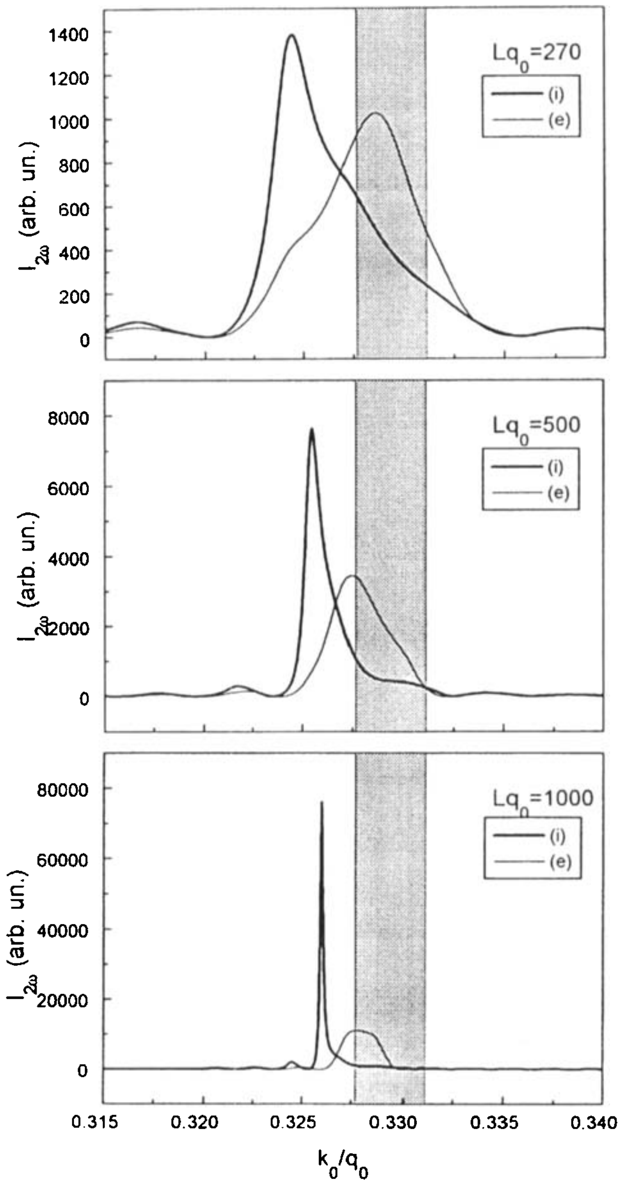

FIGURE 4 Frequency dependence of the SHG intensities related to the eigen-wave combinations (i) and (e) for different slab thicknesses.

the actual outgoing SHG intensity. This variation is evident as a relatively large spread of the data around the fitting curve in Fig. 5.

The enhancement of the SHG signal in the vicinity of the "forbidden" gap can be explained by the frequency dependence of the reflectivity of the optical waves on the boundary between the isotropic and the SmC* material. In the region $2\omega \approx \omega_B$ the reflectivity for the SHG waves corresponding to the branches 2 and 3 of the dispersion spectrum rapidly increases and reaches the value of 1 for the 2ω at the band gap[14]. The SHG beam with the frequency 2 ω close to the band edge therefore experiences many back reflections from the surfaces before it "escapes" out from the slab. For the sample of the thickness $Lk_2(2\omega) = (2N+1)\pi$ all the partially back reflected beams are in phase and so they add up together constructively. The largest enhancement appears for N=1 and is given by a factor $S = (1-R^2)^{-1}$ where R is the reflectivity of the branch 2 at $k_2(2\omega) = \pi / L$.

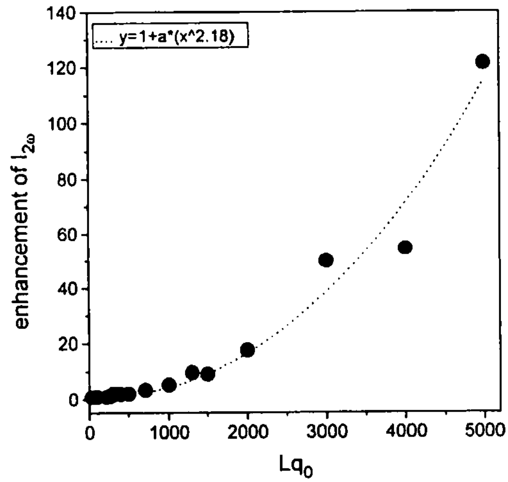

FIGURE 5 The enhancement ratio as a function of a slab thickness.

CONCLUSIONS

As mentioned in the introduction, the first attempts to experimentally observe the effects discussed in this paper has been performed by Kajikawa et al. and Furukawa al.[12,13]. By varying the helical pitch of the homeotropically aligned sample of the SmC* phase they have detected the increase of the SHG signal in the region of the selective reflection band. But on the other hand the signal almost did not change when the thickness of the sample was increased[13]. This feature might be explained by the inhomogeneity of the helical periodicity of the samples and with formation of the defects.

The achievement of a perfectly homogeneous SmC* structure and an arrangement of long interaction lengths are definitely the two most important problems related to the more detailed experimental investigations and also possible applications of this materials for the optical SHG. The problem of the longer interaction lengths might be solved by using planar instead of the homeotropic cells or by placing the SmC* material into capillaries.

A *Mathematica* package which gives exact numerical solutions for the SHG field in the case of the wave propagation along the SmC* helical axis in various experimental geometries can be found on the Internet at location: http://optlab.ijs.si/lcpro.

References

[1.] for recent review see for instance: M. Houé and P. D. Townsend, *J. Phys. D: Appl. Phys.*, **28**, 1747 (1995).
[2.] for recent review see for instance: E. Yablonovitch, *J. Mod. Opt.*, **41**, 173 (1994); J. W. Haus, *J. Mod. Opt.*, **41**, 195 (1994); J. B. Pendry, *J. Phys., Condens. Matter.*, **8**, 1085 (1996).
[3.] K. Sakoda, K. Ohtaka, *Phys. Rev. B*, **54**, 5742 (1996).
[4.] O. Parodi, *J. Physique (Paris)*, **36**, 22 (1975).
[5.] H. P. de Vries, *Acta Cryst.*, **4**, 219 (1951).
[6.] I. Drevenšek Olenik and M. Čopič, *Phys. Rev. E*, **56**, 581 (1997).
[7.] V. A. Belyakov, N. V. Shipov, *Phys. Lett.*, **86A**, 94 (1981).
[8.] V. A. Belyakov, N. V. Shipov, *Sov. Phys. JETP*, **55** , 647 (1982).
[9.] S. V. Shiyanovskii, *Ukr. Phys. Journ.*, **27**, 361 (1982).
[10.] S. V. Shiyanovskii, *Proc. SPIE*, **2795**, 2 (1996).
[11.] M. Čopič, I. Drevenšek Olenik, *Liq.Cryst.*, **21**, 233 (1996).
[12.] K. Kajikawa, T. Isozaki, H. Takezoe, A. Fukuda, *Jpn. J. Appl. Phys.*, **31**,L679 (1992).
[13.] T. Furukawa, T. Yamada, K. Ishikawa, H. Takezoe, A. Fukuda, *Appl. Phys. B*, **60**, 485 (1995).
[14] see for instance: S. Chandrasekhar, *Liquid Crystals*, (University Press, Cambridge, 1992), p. 237.